A mechanistic study of Layered-Double Hydroxide (LDH)-derived nickel-enriched mixed oxide (Ni-MMO) in ultradispersed catalytic pyrolysis of heavy oil and related petroleum coke formation

Claydon, Ryan; Wood, Joe

DOI:
10.1021/acs.energyfuels.9b02735

Document Version
Publisher's PDF, also known as Version of record

Citation for published version (Harvard):
Claydon, R & Wood, J 2019, 'A mechanistic study of Layered-Double Hydroxide (LDH)-derived nickel-enriched mixed oxide (Ni-MMO) in ultradispersed catalytic pyrolysis of heavy oil and related petroleum coke formation', *Energy & Fuels*, vol. 33, no. 11, pp. 10820-10832. https://doi.org/10.1021/acs.energyfuels.9b02735

energy&fuels

Article

Cite This: Energy Fuels 2019, 33, 10820−10832

pubs.acs.org/EF

A Mechanistic Study of Layered-Double Hydroxide (LDH)-Derived Nickel-Enriched Mixed Oxide (Ni-MMO) in Ultradispersed Catalytic Pyrolysis of Heavy Oil and Related Petroleum Coke Formation

Ryan Claydon[†] and Joseph Wood*[,†]

[†]School of Chemical Engineering, University of Birmingham, Edgbaston, Birmingham, B15 2TT, U.K.

ABSTRACT: Heavy oil contains a significantly lower H/C ratio and higher quantity of organic heteroatoms and organometallic complexes than conventional light oil. Consequently, novel catalytic materials are needed to aid in heavy oil upgrading to remove the deleterious components and support the higher demand for low sulfur and higher value fuels. Heavy oil upgrading was studied using an inexpensive nickel-aluminum Layered Double Hydroxide (LDH)-derived Ni-enriched Mixed Metal Oxides (Ni-MMO) dispersed catalyst in a Baskerville autoclave. The conditions were set at 425 °C, initial pressure of 20 bar, 0.02 Catalyst-To-Oil (CTO) ratio, and a residence time of 30 min to mimick previously optimized conditions for in situ upgrading processes. The extent of the upgrading following catalytic pyrolysis was evaluated in terms of a solid, liquid, and gaseous phase mass balance, liquid viscosity reduction, desulphurization, and True Boiling Point (TBP) distribution. A typical in situ activated CoMo-alumina commercial hydroprocessing catalyst was used as a reference. It was found that the produced oil from dispersed ultrafine Ni-MMO exhibited superior light oil characteristics. The viscosity decreased from 811 to 0.2 mPa·s while the light naptha fraction increased from 12.6% of the feed to 39.6%, with respect to the feed. Using a thorough suite of analytical techniques on the petroleum coke product, including Thermogravimetric Analysis (TGA) and Scanning Electron Microscopy (SEM), a reaction mechanism has been hypothesized for the upgrading by dispersed Ni-MMO under both N_2 and H_2 atmospheres. Under a N_2 atmosphere, the Ni-MMO, generated by the in situ thermal decomposition of the LDH, demonstrate a preferential asphaltene and poly aromatic adsorption mechanism, generating a poly aromatic mixed oxide-coke precursor. While using Ni-enriched mixed oxides under a reducing H_2 atmosphere, hydrogenation reactions become more significant.

1. INTRODUCTION

Petroleum demand is expected to grow over the coming decades before being phased out by renewable alternatives. The BP Energy Outlook[1] predicts that hydrocarbons as an energy supply will cease to grow between 2030 and 2040. However, conventional reserves are slowly depleting and with this in mind, heavy oil and bitumen resources may be able to mitigate this concern. There are an estimated 8 trillion barrels of heavy oil and bitumen remaining in Canada and Venezuela.[2] However, primary production in these petroleum reservoirs is limited by both the physical and chemical properties of the oil. These unfavorable properties constitute an excessive viscosity, which significantly limits the flow rates of production wells. Consequently, Enhanced Oil Recovery (EOR) techniques are employed to partially upgrade these heavy oils. In-Situ Combustion (ISC) and Steam-Assisted Gravity Drainage (SAGD) are examples of thermal EOR methods that have previously been employed. A number of EOR techniques have been tested in conjunction with downhole catalysts to ascertain their role in upgrading the oil in situ. High temperatures may be achieved in the reservoirs as a result of thermal techniques, with a notable example Toe-to-Heel Air Injection (THAI) leading to temperatures exceeding 450 °C and peaking up to 600 °C in laboratory simulations.[3,4] This is an adequate temperature to promote catalytic upgrading and as such has lent itself to the development of an in-well catalyst interface otherwise known as CAtayltic upgrading PRocess In-situ (CAPRI) comprising a fixed bed of hydroprocessing catalysts within the annulus of the production liner.

Additionally, surface upgrading units are used to further improve the quality of the oil including the sulfur content. This property is tied into both the overall petroleum quality and environmental legislation. For example, the United States government implemented new legislation, beginning 2017, which limited the total content of sulfur to 10 ppm in gasoline.[5] As such, it is of great importance to minimize this constituent and its consanguineous fractions. Additional performance markers highlight the proportion of valuable gasolines and distillates and petroleum coke composition.

Anionic clays, commonly referred to as Layered Double Hydroxides (LDHs), are a class of multicomponent catalysts which have been used previously in both reforming and hydrogenation reactions, as well as acting as catalytic supports.[6,7] These compounds comprise brucite-like metal hydroxide layers, octahedrally coordinated containing at least two cations with a different ionic charge. The difference in ionic charge gives rise to layers, comprised of both anions and water, between the metal hydroxide layers. Consequently, sheet-like stacks of metal hydroxides with negatively charged interlayer regions are formed to generate the overall anionic clay structure, as illustrated in Figure 1.[6,7] While there has been some use of anionic clays as

Received: August 15, 2019
Revised: October 17, 2019
Published: October 21, 2019

DOI: 10.1021/acs.energyfuels.9b02735
Energy Fuels 2019, 33, 10820−10832

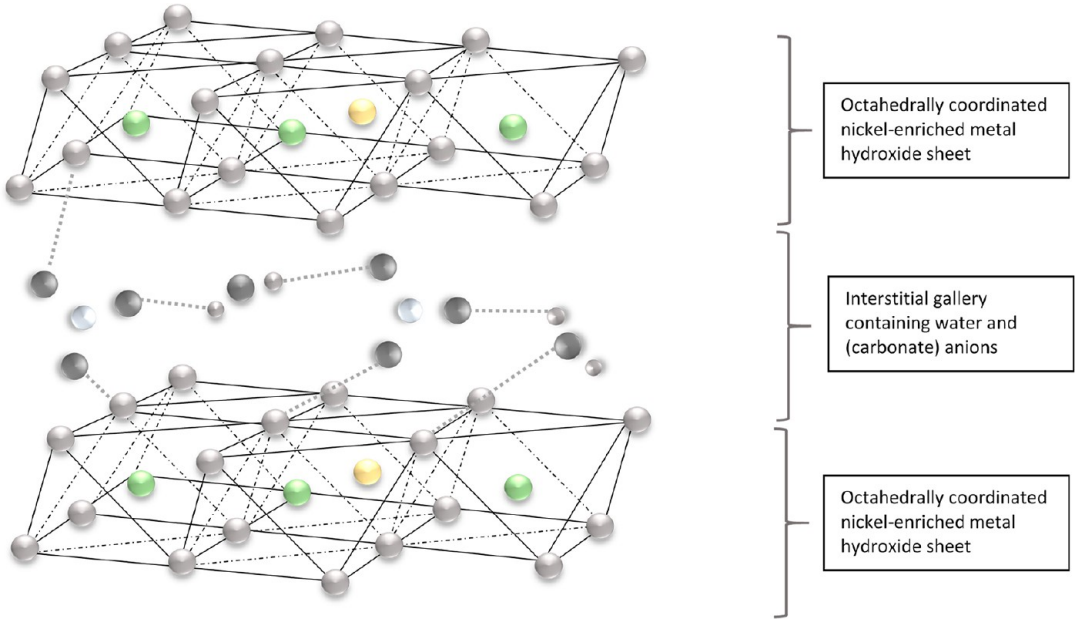

Figure 1. Graphical representation of the Layered-Double Hydroxide (LDH) prior to thermal treatment.

petroleum upgrading catalysts and additives as shown in Mostafa and Mohamed[8] and Zhao et al.,[9] much work is needed to understand the mechanism of upgrading and to realize the true potential of metal-doped anionic clays on upgrading across all facets of the upgrading products.

One critical characteristic of these anionic clays is the ability to exchange different metals into the metal hydroxide structure. This enables the tailoring of the catalyst to a specific function. For instance, a well-studied anionic clay in literature is the Mg^{2+}/Al^{3+} anionic clay in a 3:1 ratio.[6] Petroleum upgrading reactions typically use metals such as nickel, cobalt, and molybdenum.[10,11] Consequently, the substitution of nickel into the anionic clay has been chosen to tailor its use in petroleum catalytic upgrading reactions at a relatively cost-effective premium. Additionally, upon heating the layered clays lose their interstitial water and anion layers to form high-surface area mixed oxides.[6,7] This may act to release activated components into the reaction mix as well as leaving behind host sites. There are very few limitations to the nature of anions incorporated into the anionic clay structure; consequently, the vacant sites may accommodate the removal of deleterious fractions of the oil during the simultaneous upgrading and relamination of the mixed oxides.[6] The mixed oxides possess both Lewis acidic and Lewis basic sites which may sufficiently accommodate both hydrogenation and deprotonation reactions which are valuable in petroleum upgrading.[6] The thermal stability of the resultant mixed oxides which are synthesized in situ, combined with the high level of metal dispersion across the layers, also contribute to its potential viability as an upgrading catalyst.

The purpose of this study is to achieve a lower cost in situ activated alternative to hydroprocessing catalysts. The catalysts have the potential for usage in conjunction with the THAI-CAPRI as an ultradispersed catalyst reflecting a new CAPRI contacting pattern. Specifically, the study will evaluate the effect of a Nickel-Enriched Mixed Metal Oxide (Ni-MMO) catalyst derived from the in situ delamination of NiAl-LDH on heavy oil recovered from the THAI wells. The performance of the catalyst was placed into the context of both thermal upgrading and catalytic upgrading with the use of a commercial refinery catalyst ($Co\text{-}Mo/Al_2O_3$).

2. MATERIALS AND METHODS

The heavy oil used in this study was obtained from a premixed series of samples from eight different THAI production wells at Kerrobert, Saskatchewan, Canada. A representative bulk sample was taken for use during the experimentation with the properties of the heavy oil shown in Table 1.

Table 1. Properties of the Heavy Oil Feedstock Prior to Pyrolysis

Parameter	Value
Viscosity at 20 °C (mPa·s)	811
Sulfur (wt%)	3.32
Asphaltene (wt%) by nC7H16	14
ASTM D2887 Distillation	
IBP to 200 °C (%)	12.6
200 to 343 °C (%)	27.6
343 °C to FBP (%)	59.8

The LDHs were synthesized using the coprecipitation method under constant pH. Solutions containing the cation salts were dissolved in distilled water and coprecipitated into a carbonate solution. The metal salts were mixed in ratios appropriate to yield anionic clays with the desired compositions. A sodium hydroxide solution was used to maintain the optimum pH for homogeneous precipitation. Following the complete addition of the metal salt solutions, the system was left to age overnight at a constant temperature of 60 °C. The precipitate was vacuum filtrated and washed several times with distilled water. Ni/Al (3.3:1) anionic clays were synthesized using the coprecipitation method, where the metal salts were mixed in given ratios (x:y), conforming to the limits of metal ratios exhibited by anionic clays.[6] Properties of the anionic clay catalysts are shown in Table 2 with the corresponding commercial refinery catalyst properties, following extended crushing into a fine powder.

Powder X-ray Diffraction (PXRD) patterns were obtained with a Bruker D2 X-ray diffractometer using a cobalt source and nickel filter. This was used to determine the atomic arrangement of the mineral crystals. A scan speed of 30 min with a step size of 0.370 was used over a 2θ range 10−100°.

DOI: 10.1021/acs.energyfuels.9b02735
Energy Fuels 2019, 33, 10820−10832

Table 2. Results of the Nitrogen Sorption Analysis Conducted on the Ultrafine Catalysts

Catalyst2	.	Pore size (nm)	Total pore volume (cm^3/g)
Ni-Al/LDH	96.4	5.62	0.13
Co-Mo/AL2O3	198.2	6.06	0.07

Furthermore, Thermogravimetric Analysis (TGA) experiments were used to determine the chemical changes to the structure as the temperature within the reactor increases, helping to further delineate the reaction mechanism. A 22 mg portion of catalyst was added to a platinum crucible before being heated up at a rate of 10 K/min from 25 °C to the maximum temperature of 900 °C, under a constant flow set at 10 mL/min of air.

Scanning Electron Microscopy (SEM) photographs were taken to highlight the morphology of the catalyst species. The sample was mounted on a carbon disc, before being sputter-coated in gold to improve conductivity and consequently morphological resolution. This helped in the identification of the anionic clays, while highlighting the morphological differences prevalent when intercalating new metal species into the clay layers. Additionally, EDX was used to estimate the cation ratio in the brucite-like layer.

Temperature Programmed Reduction (TPR) and Desorption (TPD) was performed to evaluate the reduction temperature of the Ni-MMO. A Quantachrome ChemBet Pulsar equipped with a Thermal Conductivity Detector (TCD) was used in conjunction with approximately 20 mg of the catalyst loaded into a quartz U-tube reactor. The temperature was ramped from room temperature to 900 °C using a ramp rate of 10 °C/min while recording the intensity of H_2 uptake using a H_2 (5%) in Ar gas mix. TPD measurements were taken using the same apparatus but with a NH_3 (5%) in He gas mix. Approximately 40 mg of the catalyst was heated under He to 300 °C, before holding for 1 h and cooling to room temperature. The NH_3 (5%) in He was introduced for 2 h before switching the gas back to He and ramping from room temperature to 900 °C using a ramp rate of 10 °C/min.

For the oil upgrading reactions, a 100 mL capacity (Baskerville) stirred batch reactor, set in a removable high-temperature electrical heater, was used to facilitate the heating, agitation, and upgrading, with which parameters were selected following a previous optimization study.[12] Details of the experimental conditions are highlighted in the section Comparison of Petroleum Upgrading with Anionic Clays, Refinery-Grade Catalyst, and Thermal Upgrading.

After collecting the liquid fractions, a range of measurements were taken to analyze the quality of the product. The asphaltene content was estimated using a mixture of 40 mL of *n*-heptane (precipitating agent) and 1g of upgraded oil that was agitated constantly for 4 h. An AR 1000 (TA Instruments Ltd., UK) rheometer was used to measure the viscosity of the liquid products at temperature of 25 °C. GC method ASTM D2887 with the Agilent 6850N GC calibration mix comprising C_5-C_{44}, in addition to the ASTM D2887 reference gas oil mix No.1 Lot 2, was used to determine the percentage yield of light napthas (IBP to 200 °C), middle distillates (200 to 343 °C), and residues (343 °C+). This is a standard test method to determine the boiling range distribution of petroleum samples by gas chromatography. Total Sulfur Analysis by titration to determine sulfur wt%/wt was carried out by Exeter Analytical.

Coke quantification using the TGA curve of asphaltene and wax saturated coke particles is the commonly adopted method demonstrated in previous studies. This method makes the assumption that coke constitutes all components burnt-off at and above 600 °C rather than accounting for compositional variations in coke.[4,13−15] However, this paper sought to use a more accurate method of coke quantification and characterization. Consequently, toluene-insoluble coke precipitation and subsequent TGA of the product was employed.[16] Additionally, both elemental (CHNS) and SEM analysis were undertaken on the coke samples. This provided new insights into the mechanism of coke formation and the differences between thermal upgrading and catalytic upgrading.

3. RESULTS AND DISCUSSION

3.1. Layered-Double Hydroxide Characterization.

3.1.1. PXRD. Successful synthesis of the layered anionic clay structure was confirmed using Powder X-ray Diffraction (PXRD) analysis. The diffractogram of NiAl-LDH in Figure 2 highlights the various reflections corresponding to the crystal lattice of an anionic clay, the peaks of which having been picked and matched to a material with the same crystal lattice formulation to PDF 00-056-0953, a nickel aluminum LDH with Ni/Al 2:1 molar ratio. A slight deviation from the matched LDH reflects the difference in molar ratio between Ni and Al. The three narrow peaks occurring at low 2θ values (2θ = 14.1, 27.8, and 41.5) can be assigned to the lattice planes (003), (006), and (012). These reflect the ordering of the layered clay structure and highly crystalline nature of the clay, while the overall peak distribution accurately reflects typical anionic clay XRD patterns.[6,7]

Furthermore, to validate the process of in situ delamination of the anionic clay, during the temperature buildup of the reaction, the anionic clay was calcined at 425 °C before being reanalyzed using XRD. The subsequent delaminated anionic clay diffractogram, illustrating large broad peaks which are highly indicative of

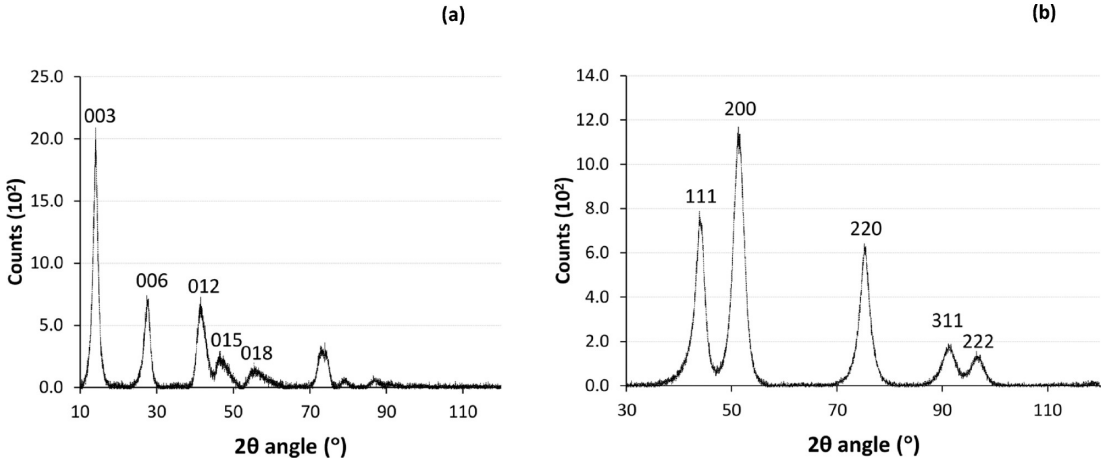

Figure 2. (a) PXRD peaks of NiAl-LDH highlighting successive 003, 006, and 012 peaks indicative of the layering in the LDH in addition to (b) PXRD of resultant mixed oxides following calcination at 425 °C.

DOI: 10.1021/acs.energyfuels.9b02735
Energy Fuels 2019, 33, 10820−10832

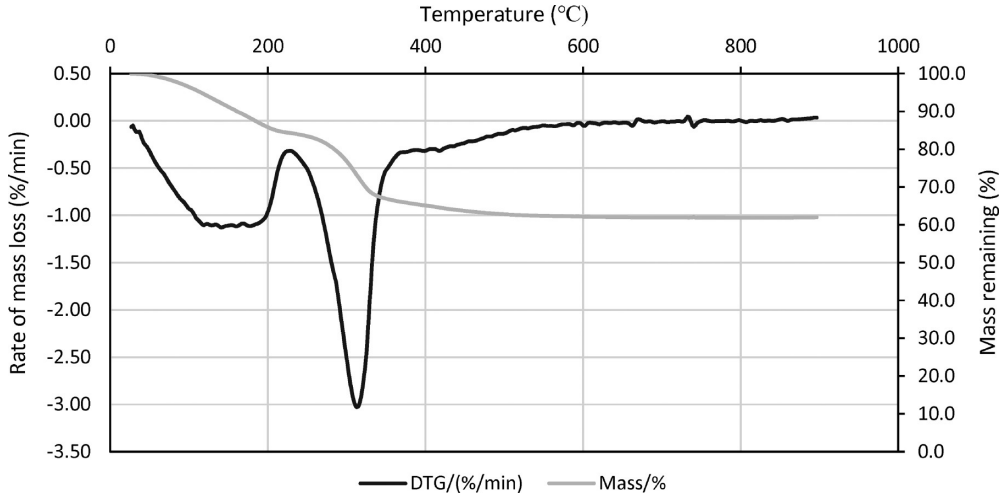

Figure 3. Thermogravimetric analysis of the catalyst prior to the upgrading reaction.

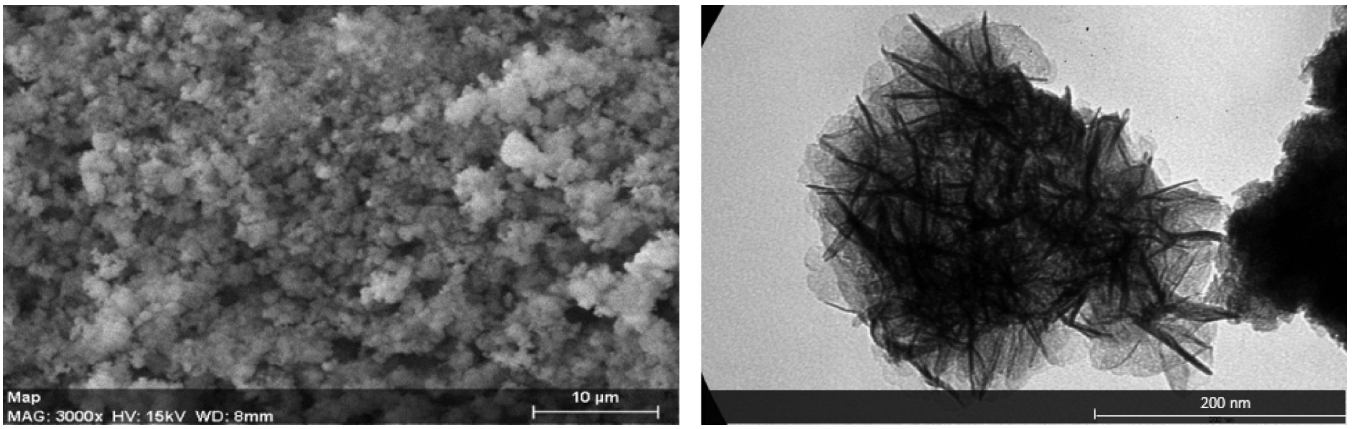

Figure 4. Scanning Electron Micrograph at a 10 μm scale (a) and transmission electron micrograph at a 200 nm scale (b) of the NiAl-LDH ultrafine catalyst powder.

an amorphous structure relating to the resultant Ni-MMO. The peaks have been picked as perfect match using the PDF 00-047-1049 for Bunsenite, a nickel oxide, while it is inferred that the poor crystallization of aluminum oxides has led to its absence in the diffractogram. They do however remain active components in the resultant mixed oxide material. Upon calcination, Ni-Al LDH forms polyphasic Ni-MMO containing a NiO phase, a quasi-amorphous spinel-type phase, and a Ni-doped alumina phase grafted to the spinel phase.[7]

3.1.2. TGA. The TGA analysis in Figure 3 highlights the thermal stability of the catalyst when subject to rising temperature. The results clearly demonstrate two zones prior to reaching 425 °C, the reaction temperature, which can be classified into dehydration and dehydroxylation stages, at approximately 100 and 250 °C, respectively, the latter of which is accompanied by decarboxylation to a lesser extent.[6,7] These peaks correspond with the XRD-post thermal treatment highlighted in Figure 2b wherein the delamination has led to the production of a high-surface area triphasic metal oxide. These layers contain active zones on which cracking, hydrogenation, and desulphurization can take place.[7] It is also thought that the liberation of water molecules and hydrogen may serve to supply an activated hydrogen donor at reaction temperature and pressure.

Furthermore, the vacant sites left by the elimination of water and carbonate in anionic clays, highlighted by the mass loss peaks in Figure 2, are known to accommodate the reuptake of other anionic and polar species.[6] This inherent property of delaminated anionic clays may therefore prove to be useful in removing deleterious species within the hydrocarbon mixture, thereby undergoing relamination to possibly form a complex anionic clay derivative.

3.1.3. SEM and TEM. The images in Figure 4 highlight the morphological structure of the NiAl-anionic clay as well as an approximation of the particle size, pertaining to approximately 1 μm crystallites, forming approximately 3 μm agglomerates. The anionic clay demonstrates a plate-like structure comprising an undulating structure with hexagonal crystallites, typical of the LDH morphology. TEM imaging better highlights the agglomeration of hexagonal plates inherent in the structure of LDHs.[6]

Results obtained from EDX in Table 3, highlights the elemental content of the material. As shown, the intercalation of Ni and Al into the brucite-like layer was confirmed with a molar ratio at 3.3:1. This demonstrates the successful enrichment of nickel into the LDH during the coprecipitation synthesis method. The carbon and oxygen represent the oxygen within the CO_3^{2-} anions, H_2O molecules, and within the −OH groups representing the brucite-like layer. It is worth noting that

DOI: 10.1021/acs.energyfuels.9b02735
Energy Fuels 2019, 33, 10820−10832

Table 3. EDX Results of Ni-Al/LDH Catalyst

Element	Atomic number	Atom (at.%)
Oxygen	8	68.56
Carbon	6	15.14
Nickel	28	12.51
Aluminum	13	3.79
		100

EDX does not detect hydrogen atoms; as a result, absolute quantification of the chemical structure cannot be confirmed.

3.1.4. TPR and TPD. Figure 5 demonstrates the peaks of reduction and extent of NH_3 desorption across the temperature range. H_2 (5%)-TPR was performed to evaluate the reduction profile of Ni-MMO. The intensity of reduction peaked at 602.6 °C, following a less intense reduction profile which peaked at 344.0 °C. NH_3(5%)-TPD was performed to investigate the acidity of the catalyst. The total number of acid sites has been calculated at 0.368 mmol/g.

A typical HDS CoMo-(γ)alumina catalyst with a similar surface area to the one used in these experiments at 204.24 m^2/g was shown to have an acid site density of 1.5134 mmol/g.[17] The significant difference in acidity between the prepared and refinery catalyst is influenced by the alumina support. This has been shown to heavily influence catalyst acidity and promote coke-generating reactions in previous work.[14]

3.2. Comparison of Petroleum Upgrading with Anionic Clays, Refinery-Grade Catalyst, and Thermal Upgrading. The upgrading experiments were performed in a Baskerville batch reactor under the following parameters; a reaction time of 30 min, Catalyst-To-Oil (CTO) ratio of 0.02 g/g, agitation speed 500 rpm, initial pressure 20 bar, and 425 °C reaction temperature with N_2 reaction gas followed by hydrogen reaction gas, denoted in the paper by (N_2) and (H_2), respectively.

3.2.1. Effect of Catalyst on Product Distribution. The preliminary steps taken within the analysis of petroleum upgrading comprise the mass balance. This is used to quantify the following three phases produced by the reactions: gas, oil, and petroleum coke (the latter containing a mixture of condensed asphaltenes, resins, waxes, and deactivated catalyst). Broad upgrading trends are subsequently identified before a more detailed analysis on the various products is discussed.

$$\text{Gas (wt\%)} = 100 - \text{liquid yield (wt\%)} - \text{solids and residue yield (wt\%)}$$

The "solids and residue yield" is subsequently split into two components following toluene washing: (i) petroleum coke (and coked-up catalyst) and (ii) liquid phase. Subsequently, TGA curves identified the amount of catalyst remaining following coke burnoff.

The normative aim concludes that the amount of oil produced should be high relative to the other phase products.[10,14] However, there is invariably a trade-off between quality and quantity that directly affects the choice of processing methods employed by a refinery. This is mostly satisfied by market factors wherein the supply and demand relationship of different quality fuels and products becomes significantly influential on the refinery processing programmes.[18]

The reaction environment is host to a great deal of reactions all of which impact both the quality and quantity of products. Cleavage of C−C, C−H, and C-heteroatom bonds generates intermediate radicals which in turn can undergo several transformations depending on the catalyst involved and reaction environment. If hydrogen is not present in large quantities at high-pressure, it is more difficult for the radicals to undergo rearrangement and termination reactions, leading to the formation of radical adducts forming. As a result, an increase in the amount of solid residue in the form of petcoke is effected.[14]

The relative proportions of the phases produced, shown in Figure 4, are used to provide a general insight into the reaction mechanisms occurring between thermal and catalytic upgrading. The general trends and corresponding interpretations are carefully considered but, at this stage, do not represent the significant differences shown by subsequent analytical techniques employed on the liquid and solid phases.

From Figure 6, it can be observed that the liquid yield decreases in the following order: thermal (H_2) > Ni-MMO (H_2) > thermal (N_2) > CoMo-alumina (H_2) > CoMo-alumina (N_2) > Ni-MMO (N_2). When using H_2 gas as a H_2 donor in the presence of catalysts, it is observed that the mass balance is distinctly altered as opposed to that using a N_2 atmosphere, which is supported in previous works.[13]

With respect to the Ni-MMO, the addition of H_2 led to a marked increase in liquid yield from 70.3 to 78.9% with consequent reductions in wt % coke from 10.4 to 6.40% and wt % gas reduction from 18.3 to 13.8%. This is significant when accounting for the average error margin across the resultant phases of only 1.78% as it clearly demonstrates the role of H_2 gas

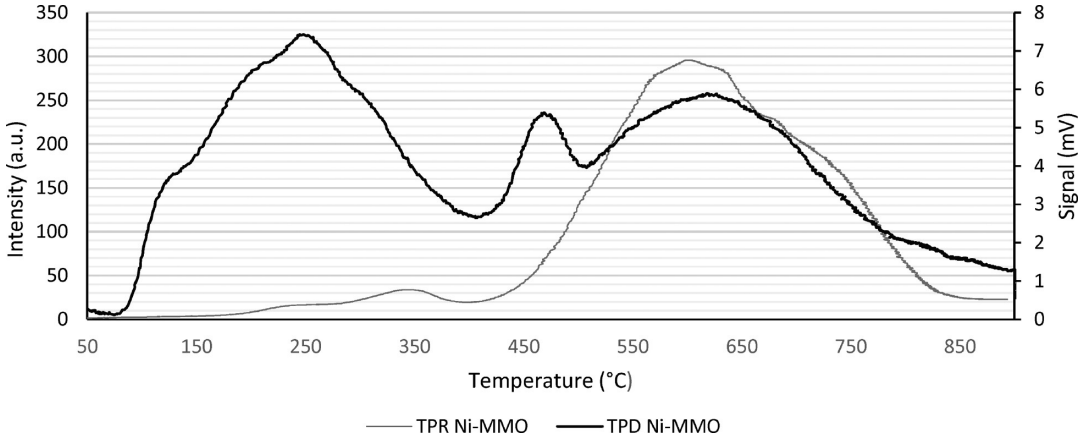

Figure 5. TPR and TPD profiles for the Ni-MMO catalyst.

DOI: 10.1021/acs.energyfuels.9b02735
Energy Fuels 2019, 33, 10820−10832

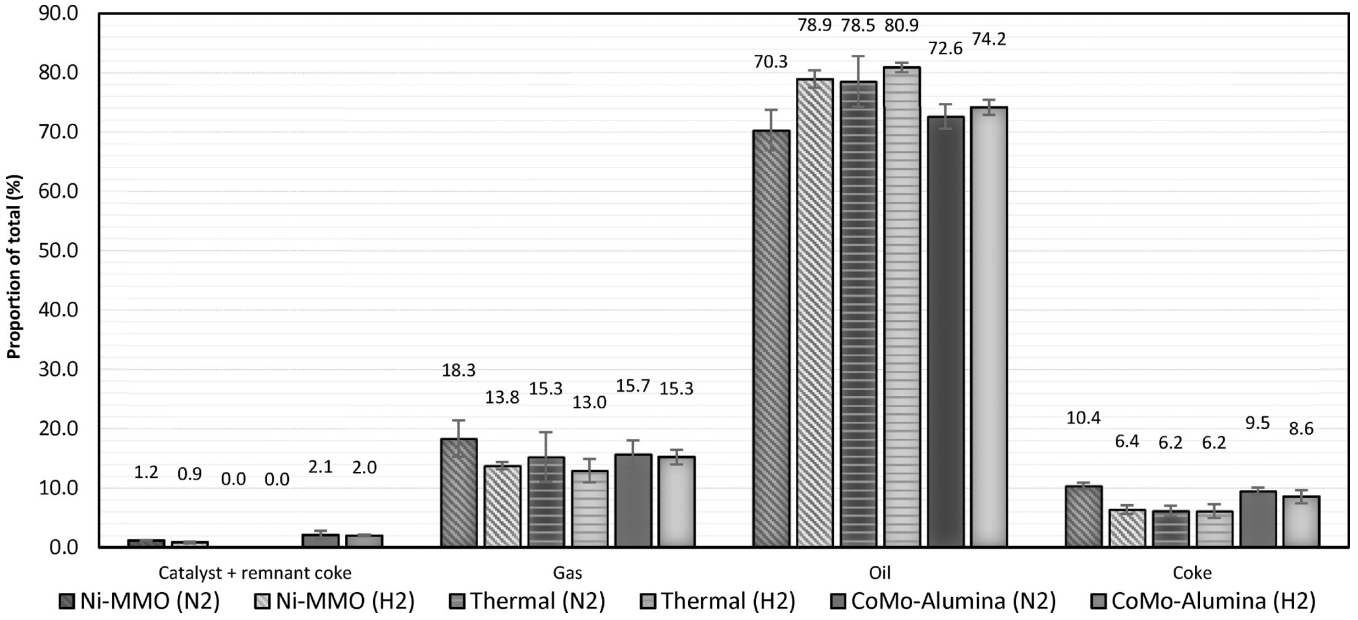

Figure 6. Mass balance following upgrading reactions highlighting coke, oil, gas, and catalyst + remnant coke.

as an active hydrogen donor in hydrogenation reactions and consanguineous coke suppression roles.

When using a CoMo-alumina catalyst, the addition of H_2 led to a marginal increase in liquid yield from 72.6 to 74.2% with consequent reductions in wt % coke from 9.5 to 8.6% and wt % gas reduction from 15.7 to 15.3%. Combined with the error margin, the catalyst has made a minimial impact on the mass balance under different gas regimes.

It is shown that both the Ni-MMO (N_2) and CoMo-alumina (N_2) give rise to elevated quantities of petroleum coke relative to the other reaction conditions. In particular, the thermal upgrading regimes both generated the least amount of coke at a steady 6.2%.

The acid site-containing alumina within the CoMo-alumina catalyst structure leads to acid-catalyzing C−C and C-heteroatom cleavage.[11,19] Under a N_2 atmosphere, it is difficult to cap the resultant free radicals because active H· is scavenged from the mixture rather than being freely available under a H_2 atmosphere. Under a N_2 environment, carbon rejection is predominant while activated hydrogen is redistributed among the hydrocarbon molecules.[20] The increase in liquid fraction by 1.6% for CoMo-alumina under a H_2 relative to N_2 atmosphere highlights the effect of hydrogenation on the product yield.

While the Ni-MMOs yield the largest quantity of petroleum coke at 10.4% under N_2, the theory behind this is decidedly different. Initial interpretations indicate that the condensation of radicals to petcoke is accommodated by the uptake of polarized asphaltenic and resinous radicals by the positively charged metal oxide sheets to ultimately generate polyaromatic-saturated layered structures—a pseudomorph of the initial anionic clay layered structure prior to heating. This theory is highly plausible given that interstitial anions present within anionic clays can have widely complex structures including complex organic and organometallic forms, while the mixed oxides have a strong tendency to reproduce the original layered structure when in solution.[6] NiO nanoparticles have previously demonstrated active asphaltene sorption sites, which is later supported by analyzing the asphaltene content of the upgraded liquid and sulfur content of the petroleum coke.[21] The asphaltene-saturated active sites may then be responsible for a multitude of side reactions culminating in the production of adducts as a coke-precursor. Under a H_2 environment, the yield of coke dropped significantly by 4% (0.52% and 0.59% error for N_2 and H_2 atmosphere-derived coke, respectively). The Ni-MMO undergoes in situ partial reduction during the heat-up phase to 425 °C (under a 100% H_2 atmosphere), thereby contributing to the hydrogenation function. Fast-diffusing active hydrogen species led to an increase in hydrogenation and hydrocracking reactions. Specifically, free radicals generated by the carbon rejection routes are capped-off thereby inhibiting the condensation reactions which leads to petroleum coke formation.[22]

The thermal regimes both generated the least amount of coke at 6.2%. The 2.4% difference in yield of liquid between the two reaction environments was accommodated by the yield of gaseous products, with which thermal (N_2) demonstrated overcracking into smaller gaseous hydrocarbon molecules due to the unavailability of active hydrogen. Without metallic active sites and a support, the magnitude of both hydrogenation and cracking is limited, hence there was no difference in the coke production between N_2 and H_2 gas atmospheres. This also explains why the alumina-supported CoMo catalyst produced a higher amount of coke in both the N_2 and H_2 regimes, yielding an additional 3.3 and 2.4% of coke for CoMo-Alumina (N_2) and (H_2) over the thermal regime counterparts. The increased amount of carbon rejection pathways leading to free radical generation and condensation, accommodated by the acid-cracking alumina. This can culminate in an increase in free radical condensation and simultaneous pore blockage in the catalyst, therefore enhancing the coke quantity. Moreover, this is supported by previous studies wherein one such example alumina produced the greatest quantity of coke in comparison to Pd-doped alumina and Pd-doped carbon again demonstrating the significance of the acid-catalyzing role of alumina in upgrading.[14]

Overall, the mass balance is a useful tool in obtaining an initial understanding of the upgrading process. Ultimately, the aim is to generate most significant amount of liquid phase with the smallest possible gas and coke phases. However, it is clear that

DOI: 10.1021/acs.energyfuels.9b02735
Energy Fuels 2019, 33, 10820−10832

the Ni-MMO catalyst has a complex impact on reaction pathways such that more gas and coke is produced at the expense of the liquid phase. However, subsequent analysis on the products show distinct differences in the quality of the liquid and solid phases between the catalysts and thermal upgrading reactions which form the basis of an initial mechanistic understanding of Ni-MMO in heavy oil upgrading.

3.2.4. Effect of Catalyst on Liquid Fraction Sulfur. In terms of heavy oil, the sulfur content is a deleterious component which is typically removed using hydrotreating reactors at the refinery. Its significance rests on the fact that oils with a greater density and viscosity typically contain higher amounts of sulfur, as the higher boiling fractions are usually enriched in sulfur species.[10,23] Furthermore, the combustion of oils with high sulfur contents produce sulfur oxides and derivatives. The damage to the environment caused by such pollutants remains a big challenge for global environmental agencies. As such, maximum sulfur reduction achieved by upgrading facilities is necessary to conform to ever more strict environmental regulations.[5]

The quantity of sulfur within the liquid oil is crucial in understanding the relative upgrading mechanism of the catalyst. The amount of sulfur can correlate most closely with the relative proportion of polyaromatic hydrocarbons, since it is these molecules which constitute heteroatoms of this type.[24]

It is clear from the results in Table 4 that desulphurization is enhanced by the catalysts. The results show an obvious trend

Table 4. Sulphur Analysis of Liquid Phase

Catalyst Condition	Sulfur % wt/wt	Reduction w.r.t feed (%)
Feed Oil	3.32	
Thermal (N_2)	2.44	26.5
Thermal (H_2)	2.57	22.6
Ni-MMO (N_2)	2.27	31.6
Ni-MMO (H_2)	2.31	30.4
CoMo-A (N_2)	2.31	30.4
CoMo-A (H_2)	2.07	37.6

emphasizing sulfur removal following upgrading of the oil. To begin with, referring to the thermal (N_2) and thermal (H_2) conditions, sulfur reduction relative to the feed was 26.5 and 22.6%, respectively. There is a discernible difference of 3.9% favoring sulfur reduction in the absence of H_2. During the H_2 donor gas condition, the long-chain polyaromatic hydrocarbon components are thought to be capped off by activated hydrogen species, thereby preventing the extent of overcracking and subsequent generation of hydrocarbon gases. Consequently, there remains a higher yield of the residue fractions, supported by subsequent simulated distillation data, and therefore a higher yield of polyaromatic components which contain a significant portion of the sulfur heteroatoms. This is in broad agreement with the mass balance which highlights an increase in liquid yield at the expense of the gas yield under a H_2 gas atmosphere.

The Ni-MMO follows a similar pattern but demonstrates more significant desulphurization. Ni-MMO catalyst achieved 31.6 and 30.4% reduction relative to the feed for N_2 and H_2, respectively. What is indicated is that under a N_2 atmosphere, the triphasic metal oxide sheets favor asphaltene removal and, by extension, sulfur removal given the higher abundance of heteroatoms in asphaltenes, from the liquid phase.[24] While under a H_2 atmosphere, the petcoke formation is limited by the active hydrogen availability and polyaromatic removal is inhibited by the reduction and potential in situ sulphidation of the metal sites. A higher yield of middle distillates and residue fractions at the expense of light napthas is attained which proves that the amount of hydrogenation of higher molecular weight species increased. With this, an increased percentage of sulfur-bearing aromatics is likely to have been maintained in the liquid phase relative to the inert environment. Nonetheless, even under hydrogenation conditions, the significance of using Ni-MMO is apparent. Relative to thermal upgrading, Ni-MMO achieved a further reduction in sulfur relative to the feed oil by 5.1 and 7.85% for N_2 and H_2 atmospheres, respectively.

A difference of 4% in the petcoke produced between Ni-MMO (H_2) and Ni-MMO (N_2) has already been noted in the mass balance analysis. The highest amount of petcoke produced, at 10.4%, coincides with a reduction in sulfur, at 31.6% relative to the feed oil. Consequently, this may corroborate the idea that the sulfur is being transferred into the petcoke through polyaromatic sorption reactions rather than HDS, the reaction mechanism of a typical refinery catalyst such as CoMo-alumina. This is again demonstrated by the fact that the Ni-MMO (N_2) reaction regime favored the lowest yield of asphaltenes.

When CoMo-alumina is utilized in conjunction with H_2 gas, a significant increase in desulphurization is apparent, a 37.6% reduction, pertaining to the HDS function of the in situ activated cobalt and molybdenum species. The trend between N_2 and H_2 environments is reversed. Under a H_2 environment, the removal of sulfur is accommodated by the liberation of hydrogen sulfide gas, owing to the HDS mechanism involving the sulfide-molybdenum slabs promoted by cobalt which is demonstrably a more effective desulphurizing agent.

3.2.2. Effect of Catalyst on Viscosity and Asphaltene Content. It is clear that viscosity plays an instrumental role in assessing the value of the hydrocarbon oil. Ultimately, a high viscosity oil is difficult to transport as it contains a higher proportion of heavier, higher boiling point hydrocarbon fractions. Heavy oils are typically defined as oils with a viscosity greater than 200 mPa·s which can extend up to 10000 mPa·s, above which they are often defined as bitumen (derived from oil sands).[25] Where necessary and economically feasible, diluents such as napthas and condensates are used to reduce the viscosity to below a typical maximum pipeline viscosity of 400 mPa·s.[26] Consequently, any hydrocarbon upgrading process will aim to achieve a significantly lower viscosity relative to the feed oil. The viscosity of the oil however is interdependent on a number of factors which will be subsequently explored.

Asphaltenes should contribute toward the viscosity of an oil with the greatest significance.[27] While the specific molecular architecture of asphaltenes remains highly diverse and poorly understood, asphaltenes are thought to compose polyaromatic cores with peripheral-aliphatic chains and contain both highly polar and nonpolar groups.[21,24,28] The presence of asphaltenes in oil may lead to colloidal aggregates, a phenomenon leading to high viscosity of the oil and consequent problems such as wellbore and pipeline clogging. They are, however, nominally designated as macromolecules precipitated by a given solvent during their extraction, e.g., *n*-heptane precipitation (ASTM D4124). The generalization exists because they are highly complex and can differ in structure greatly.

The feed oil viscosity of 811 mPa·s is greatly reduced by thermal upgrading to 7.5 mPa·s. This represents a huge reduction relative to the feed oil, which is highly beneficial to the sweep efficiency and production during its recovery and subsequent transportation. However, when using the catalysts

DOI: 10.1021/acs.energyfuels.9b02735
Energy Fuels 2019, 33, 10820−10832

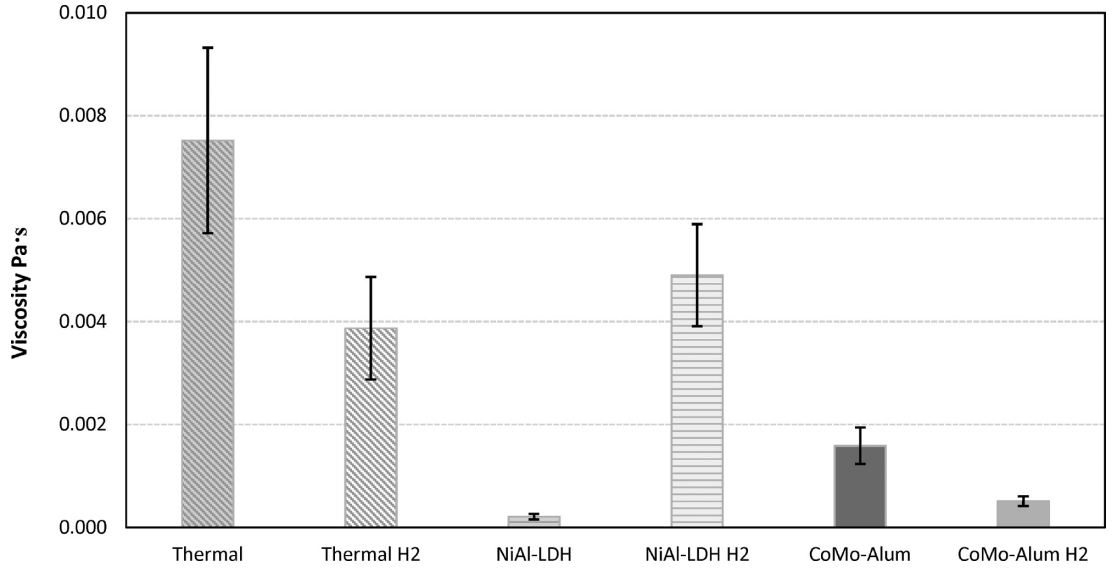

Figure 7. Viscosity of the upgraded oil as a function of catalyst type.

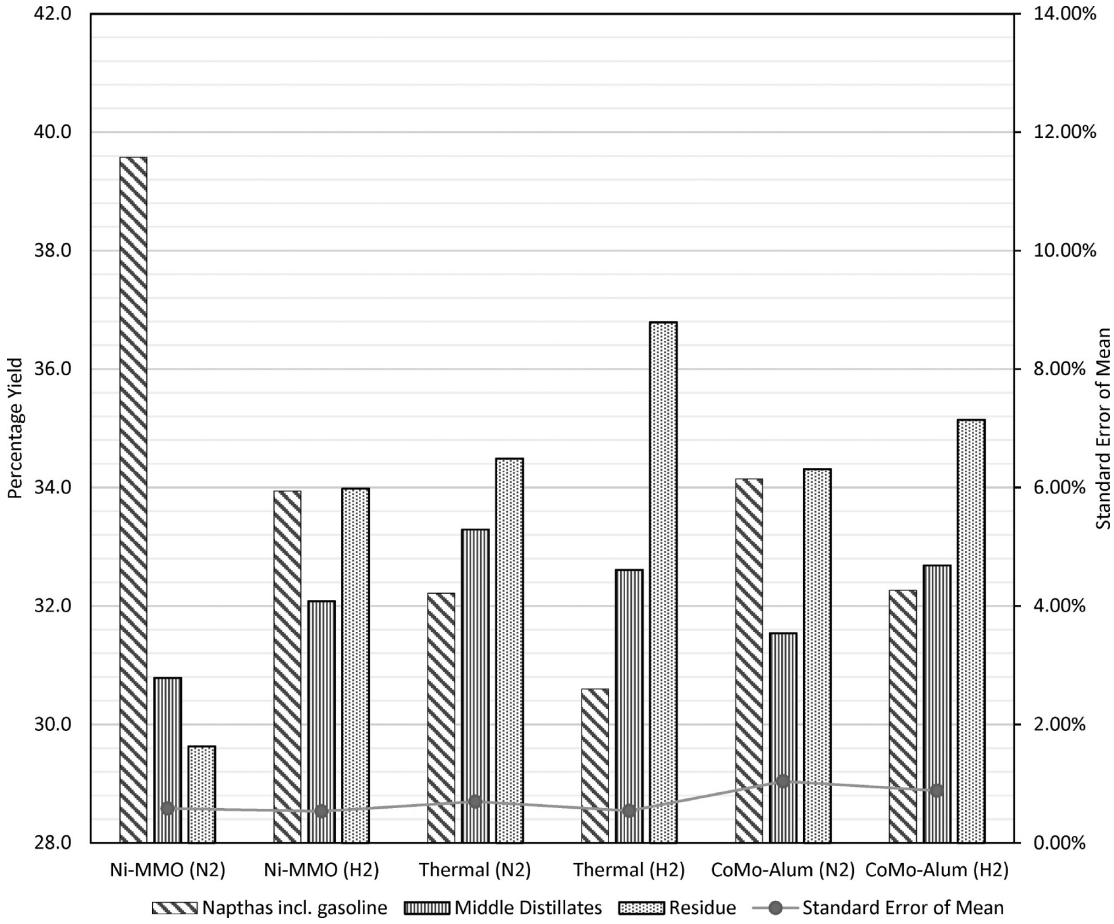

Figure 8. Distillate fractions by boiling point of upgraded liquid oil.

under a N_2 atmosphere, the viscosity reduction increases further to 0.2 and 4.3 mPa·s for Ni-MMO and CoMo-alumina, respectively. Interestingly, when a H_2 reaction gas is added there is a conflicting relationship yielding a reduction in a further reduction in viscosity to 3.9 and 4.3 mPa·s, with respect to thermal and the CoMo-alumina catalyst, but an increase in viscosity to 4.9 mPa·s for the Ni-MMO catalyst (see Figure7).

It must be noted that the comparatively small standard deviation with respect to Ni-MMO (N_2) corresponds to the fact that the viscosity generated is nearly 2 orders of magnitude less than the viscosity generated by Thermal (N_2). Taking this into account, the error is consistent with the other conditions.

It is clear that the liquid produced using Ni-MMO reflects chemical structures that allow the liquid to flow more easily.

DOI: 10.1021/acs.energyfuels.9b02735
Energy Fuels 2019, 33, 10820−10832

More to the point, the catalyst which produced the lowest yield of asphaltenes was Ni-MMO (N_2), with an average of 5.4%, while CoMo-Alumina (N_2) and thermal (N_2) yield averaged 6.4% and 7%, respectively. In previous research, the role of anionic clays has extended to aromatic removal.[8] Consequently, the role of collapsed (delaminated) anionic clays may extend to adsorbents of asphaltenes. It has been demonstrated previously that a significant increase in asphaltene adsorption onto nanoparticulated alumina occurs with an increasing NiO loading, suggesting it could be a valuable in situ upgrading material for asphaltene removal.[28] This explanation justifies a possible reaction mechanism for a decrease in viscosity following in situ delamination of Ni-MMO, which produces several nickel and aluminum oxide phases. The increase in viscosity following the addition of H_2 as the reaction gas falls in-line with the increased asphaltene content of the oil. Under a H_2 environment, the asphaltene content was as follows: 10, 4.4, and 6.7%, for Ni-MMO, CoMo-alumina, and thermal, respectively. As such, it may be prudent to distinguish between two predominant roles of the Ni-MMO additive under both reaction gases. First, under a N_2 atmosphere, the role of an asphaltene sorbent may be more significant, while under a reducing atmosphere of H_2, the hydrogenation reaction pathway may be more prominent, albeit less significant compared to a typical HDS catalyst. This latter pathway is thought to cap the asphaltic radicals with activated hydrogen at the relevant metal active sites. This pathway can therefore be recognized as a method to suppress coke formation, which is proven by the corresponding mass balance, at the expense of having higher resistance to flow through pipelines and a higher asphaltene content which is deleterious to pipeline infrastructure.

3.2.3. Effect of Catalyst on Distillate Products. Figure 8 highlights the relationship between percentage yield and TBP, achieved using an Agilent 8950 GC under a C7−C44 calibration mix anda reference gas oil mix. When a heavy oil has been upgraded, either thermally or catalytically, the expectation is that higher boiling point fractions are converted into lower boiling point fractions. Accordingly, an expected shift to the left will be observed on percentage yield vs boiling point graph, thereby demonstrating a higher yield for the lower boiling point components.

Simulated distillation results from Figure 8 highlight the following naptha (gasoline) fraction trend: Ni-MMO (N_2) > CoMo-alumina (N_2) > Ni-MMO (H_2) > thermal (N_2) > CoMo-alumina (H_2) > thermal (H_2). The middle distillate fractions highlight the trend: thermal (N_2) > CoMo-alumina (H_2) > thermal (H_2) > Ni-MMO (H_2) > CoMo-alumina (N_2) > Ni-MMO (N_2). Finally, the residue trend highlights: thermal (H_2) > CoMo- alumina (H_2) > thermal (N_2) > CoMo-alumina (N_2) > Ni-MMO (H_2) > Ni-MMO (N_2).

If this data is placed into the context of asphaltene content from Ni-MMO-derived liquid phase, what is shown is a clear correlation. With a lower asphaltene content, a higher yield of comparatively lighter molecules is produced. This is justified due to the relatively high boiling point of asphaltene macromolecules and the LDH's role of removing polyaromatics. Consequently, this corroborates the hypothesis that Ni-MMO (N_2) favors an upgrading reaction pathway as a polyaromatic sorbent due to the abundance of NiO sites. When drawing a comparison between Ni-MMO (N_2) and Ni-MMO (H_2), the results support the idea of abundant free radical stabilization under a H_2 atmosphere. The notable increase in middle distillates by 1.3% and residue by 4.4% under H_2 supports the idea that active hydrogen species have been abstracted by the catalyst, stemming condensation reactions between hydrocarbon radicals and thereby inhibiting the formation of mesophase and subsequently petroleum coke. Furthermore, with reference to the mass balance results using Ni-MMO, under a H_2 atmosphere, the liquid yield increased from 70.3 to 78.9% that further demonstrates the significance of activated hydrogen abstraction in inhibiting coke formation. It should, however, be noted that the fraction distribution is very similar to the distribution when using CoMo-alumina as the active catalyst. Given that the asphaltene content, however, was significantly higher than both the CoMo-alumina and thermal upgraded oil under the same conditions, it also signifies the importance of the different upgrading mechanism prevalent with the Ni-MMO catalyst compared to thermal upgrading.

When using the CoMo-alumina catalyst, again a similar but less significant correlation highlights an increase of middle distillates, by 1.2%, and heavy residues, by 0.8%, at the expense of light napthas when using a H_2 reaction gas. Consequently, a similar hypothesis may be applied, indicating that wide-scale free radical termination was achieved under a H_2 atmosphere due to the abundance of active hydrogen species, while cracking was predominant under a N_2 atmosphere owing to the acidic sites present in the alumina support. The latter reaction condition consequently yielded more light napthas, accompanied by a higher yield of coke, due to overcracking and limited radical stabilization,[14] which is correctly highlighted in the mass balance.

Under a thermal reaction regime, the higher boiling point products are favored when using H_2. This a result of activated hydrogen acting as stabilizing agents following C−C cleavage of the larger hydrocarbon molecules. Under a N_2 atmosphere, the lack of H_2 accelerates overcracking reactions leading to a higher proportion of light napthas and gaseous products, the latter of which is demonstrated by the mass balance.

3.3. Effect of Catalyst on Petroleum Coke. The following sections outline characterization of the solid component using elemental analysis, SEM images, and thermal stability of the coke. The properties of coke produced from the upgrading of hydrocarbon liquids are important to study as they can highlight a preferential reaction pathway for particular catalysts and operating conditions. Furthermore, from a refinery perspective, there are important economic implications governed by the coke properties. Various different coke morphologies exist including shot-type, associated shot-type, sponge-type, and acicular-type.[29,30] Depending on its grade, the coke may have value as fuel-grade, i.e., blended with coal for use in power plants and also for use as electrode materials in aluminum manufacture. Additionally, there has been interest in using activated high-sulfur petroleum coke as a natural gas adsorbent to minimize the economic constraints on the transportation of natural gas, accommodated by cost-intensive technologies such as Compressed Natural Gas (CNG) or Liquified Natural Gas (LNG).[31] Second, the morphology of the coke produced can also affect the process capacity of a refinery.[29] Shot-coke forms spherical-ellipsoidal shaped particles that are easily removed from units such as the delayed coker drums, which can have a significant benefit on process economics.

3.3.1. Elemental Analysis (CHNS). Elemental analysis of the resulting petroleum coke particles was studied once they were thoroughly washed with toluene solvent and vacuum-dried to dissolve and remove all of the liquid hydrocarbon components. Elemental analysis of the solid residue left behind led to

DOI: 10.1021/acs.energyfuels.9b02735
Energy Fuels 2019, 33, 10820−10832

significant insights into the chemical reactions taking place during upgrading (see Table 5).

Table 5. Elemental Analysis of Coke Phase, Obtained from CHNS Combustion Tube Experiments

Sample	Carbon (wt %)	Nitrogen (wt %)	Hydrogen (wt %)	Sulfur (wt %)	Hydrogen/carbon ratio
Thermal (N_2)	89.4	1.39	4.89	4.71	0.055
Thermal (H_2)	88.4	1.58	6.63	5.40	0.052
Ni-MMO (N_2)	85.7	1.38	4.54	8.39	0.053
Ni-MMO (H_2)	84.3	1.61	4.46	9.62	0.053
CoMo-A (N_2)	88.1	1.56	4.94	5.43	0.056

A significant trend given in the table above highlights the wt % of sulfur per unit mass of petcoke produced during the upgrading. The wt % of sulfur reduces in the following order Ni-MMO (H_2) > Ni-MMO > CoMo-alumina (H_2) > thermal (H_2) > thermal (N_2).

The increased sulfur content in the petcoke substantiates previous proposed mechanism of liquid desulphurization in the presence of Ni-MMO, drawing parallels with Lakhova et al.[32,33] Once the removal of anions and interlayer water has been achieved, the LDH is subsequently left with positively charged metal oxide layer in the form of Ni-MMO. The polyaromaticity of the oil is responsible for high polarity in heavy oils, largely in itself produced by heteroatoms such as sulfur. While Mostafa and Mohamed[8] have previously witnessed a role of CoMo-LDH as an additive to remove sulfur and polyaromaticity in heavy oils, the generation of Ni-MMO may provide this reuptake of sulfur-

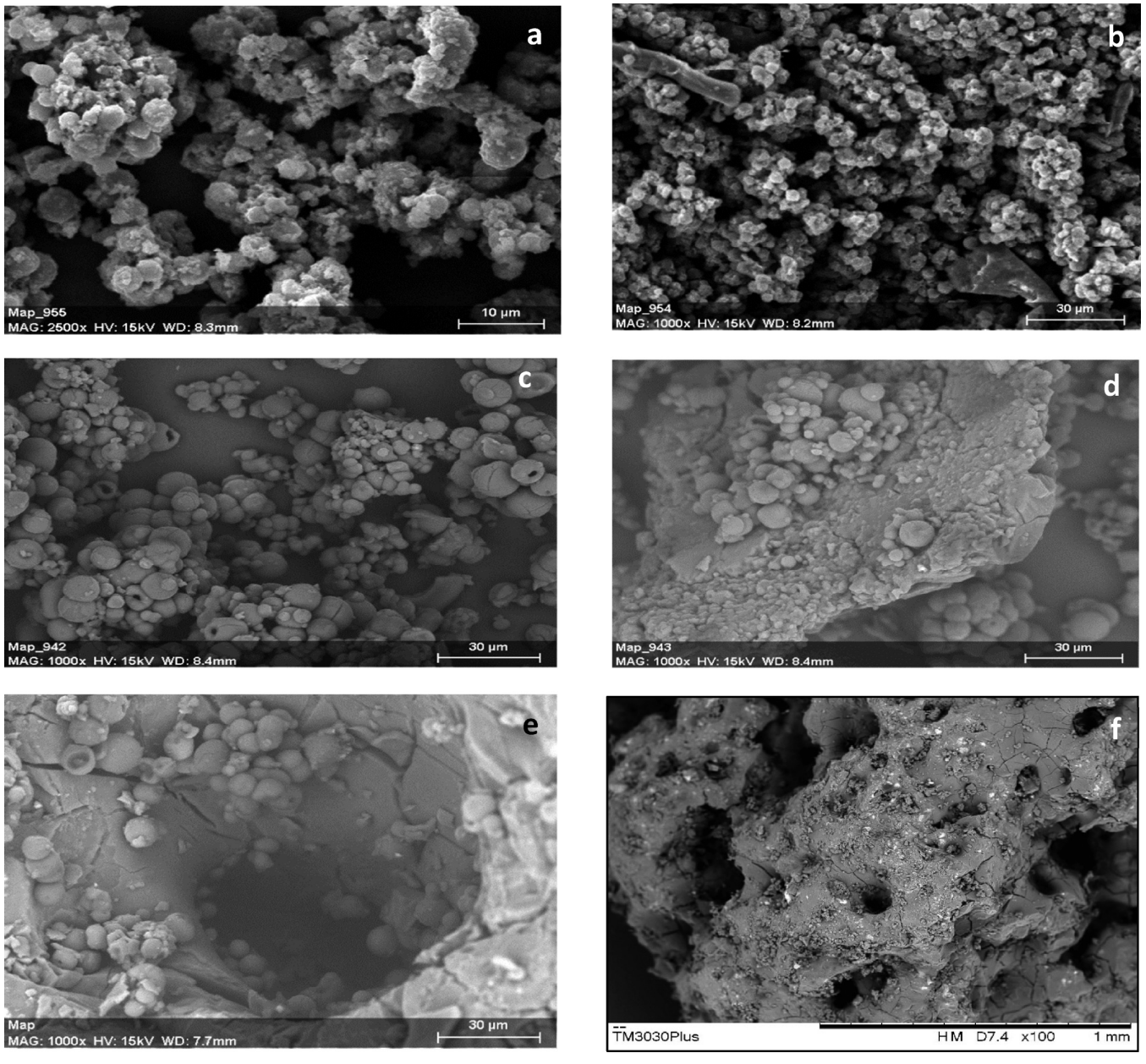

Figure 9. SEM of petcokes with respective magnifications: (a) NiAl-LDH at ×2500, (b) NiAl-LDH at ×1000, (c) thermal at ×1000, (d) thermal at ×1000, (e) CoMo-alumina at ×1000, (f) CoMo-alumina at ×100.

DOI: 10.1021/acs.energyfuels.9b02735
Energy Fuels 2019, 33, 10820−10832

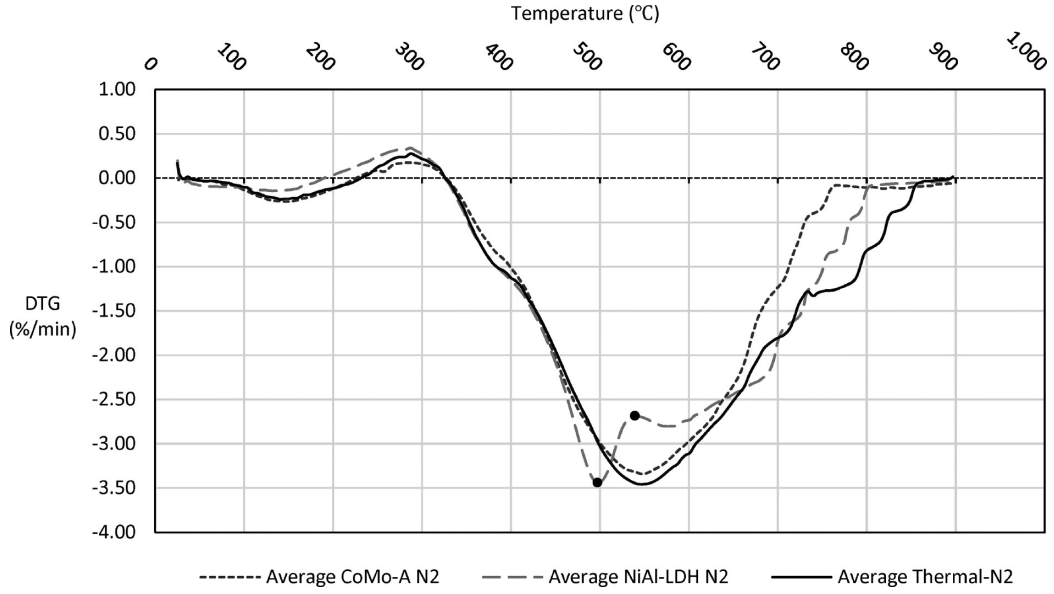

Figure 10. Thermogravimetric analysis of the produced coke after residue and asphaltenes have been dissolved out using toluene and subsequent drying under vacuum filtration.

containing polyaromatics. The collapsed clay nuclei may subsequently agglomerate to form Ni-MMO and polyaromatic-containing epicenters that function to activate and remove additional deprotonated thiophenic-type components within the oil, thereby forming large petcoke composites enriched in sulfur species.

The slightly higher percentage of sulfur present in the coke produced during Ni-MMO under a H_2 atmosphere responds to the fact that as a percentage, the amount of coke produced was much lower and therefore the higher molecular weight sulfur becomes a more significant fraction. Given that the petcoke produced from the Ni-MMO (N_2) and (H_2) was 10.4% and 6.4%, of the total reaction products, respectively, it can be calculated that the total quantity of sulfur in this coke is 0.87% and 0.62%, respectively, when using the wt % data from the elemental analysis. Therefore, it can be deduced that the sulfur-containing components are preferentially removed from the reaction mixture by the Ni-MMO under N_2. While under a H_2 atmosphere, partial reduction of the mixed oxides may partially inhibit this fixing of sulfur species into the petcoke, while promoting the capping of asphaltic radicals. It has been reported that metal oxide catalysts have been used successfully in asphaltene sorption.[21] This is in agreement with the reduced quantity of asphaltenes, middle distillates, and residue fractions, in addition to the lower viscosity when using Ni-MMO under a N_2.

Looking at the H/C ratio, a slight decrease can be noticed from thermal upgrading to catalytic upgrading when using Ni-MMO (N_2). This is interesting as it is well-known that the coking process contributes to the transfer of hydrogen from the condensing residues and asphaltenes.[10] The results therefore indicate that when using the Ni-MMO there is increased efficiency in the transfer of the hydrogen. This agrees with the presence of Lewis basic O^{2-} active sites on the Ni-MMO. This thereby improves the quality of the oil and corroborates with the viscosity data.

3.3.3. Morphology of Petroleum Coke. Analyzing the SEM images of the petcoke, shown in Figure 9a–d, it is clear that thermal and Ni-MMO-derived coke types comprise these small (semi)spherical coke particles, indicating the formation of shot-type coke. However, the CoMo-alumina-derived petcoke demonstrates a large proportion of mm-scale sponge-type properties. A highly fractured morphology with a multiplicity of pores and bubbles can be seen in Figure 9e,f, lending itself to the sponge-type coke classification.

Shot-type of coke is typically formed in delayed coker units. In this instance, it is thought to be formed when both existent and cracked light ends volatilize during the upgrading, leaving a suspension of spherical-shaped heavy tar droplets. The highly exothermic reaction of asphaltene polymerization is thought to contribute the heat required to generate this coke classification, while aided by the turbulent conditions resultant from high fluid velocities under agitation.[30] The viscosity of the droplets increases dramatically forming immature coke balls; they fail to reintegrate into the bulk liquid phase essentially fixing this macroscopic phase of petcoke. While under thermal upgrading, it is expected that shot-type coke is produced; the generation of similar petcoke under Ni-MMO highlights an economic advantage over the coke produced by CoMo-alumina. Furthermore, the mechanism of coke formation clearly diverges from conventional catalyst, which can be summarized as the fixing of larger polyaromatic compounds out of solution into the Ni-MMO-polyaromatic hybrid epicenters, accommodating an intense pseudocoking reaction.

The SEM images in Figure 9 highlight slight differences in morphological texture between the two shot-type petcokes. Bonding between a proportion of the particles is produced under thermal upgrading. This is suggestive of bonded or matrix-shot according to Siskin et al.,[29] whereas under Ni-MMO catalyst treatment, the coke appears mainly as agglomerated or clustered coke. An additional difference between Ni-MMO and thermal petcoke presides over the relative morphological smoothness of the particles. Looking at the thermal-derived petcoke images, the particles are highly spherical with relative smooth surfaces, while the particles generated with the Ni-MMO catalyst, although they too resemble microspheres, are observed as less rounded with a rougher surface morphology. This is suggestive of the difference in C/H and C/S ratios highlighted in the elemental analysis.

DOI: 10.1021/acs.energyfuels.9b02735
Energy Fuels 2019, 33, 10820–10832

Ibrahim[30] reviews the form of carbon comprising the shot-type coke, highlighting its lenticular concentric pattern giving rise to nonlinear, rounded microstructures. However, if the sulfur content is particularly high via adsorbed sulfur and related polyaromatic species, this may disrupt the smooth nonlinear pattern, thereby generating rough structures forming semi-spherical coke particles.

3.4. TGA of Produced Petroleum Coke. Figure 10 demonstrates the relationship between change in mass (%), temperature (°C), and rate of mass change when the petcoke is exposed to ramping temperature up to 900 °C at a rate of 10 °C/min in the presence of air. What can be observed are clear thermal decomposition curves generating gaseous products. There is an obvious difference between burnoff curves relating to the catalyst condition. The difference in burnoff curves is suggestive of the structures present within the petcoke samples. When assessing the peaks on the rate of mass loss curves, the peaks for thermal upgrading is much broader, indicating that certain species prevalent within this petcoke require a higher temperature for oxidation.

A clear observation is the symmetry of the thermal and CoMo-alumina burnoff curves, while that of the Ni-MMO-derived coke yields an alternative burnoff curve profile. The mass loss curve representing this latter catalyst condition peaks sharply at 498 °C before undergoing a sharp reduction in the rate of mass loss from a peak of −3.44%/min to approximately −2.68%/min. The consistency of the Ni-MMO-derived curve is highlighted by the standard deviations for both the temperatures and rates of mass loss for the distinct peak and subsequent inflection over the three repeats. These points are indicated by the successive black circles in Figure 10 with the standard deviations calculated at 8.94 °C, 0.21%/min and 6.75 °C, 0.2%/min, respectively. Additionally, this mass loss curve is shifted to the right from 638 °C, relative to the CoMo-alumina-derived curve. This relates to the fact that a higher proportion of the petcoke components is present which have a higher oxidation temperature. Organic sulfur in the petcoke can be present in many forms. Thiophenes are typically responsible for a large proportion of the sulfur content and are attached to the aromatic skeleton of the petcoke. Sulfur may also be present as side-chains of polycyclic-aromatics and napthenic molecules. However, the inorganic sulfur can be present on the coke surface.[32] The abundance of sulfur in the Ni-MMO-derived petcoke poses an explanation for the differences in these burnoff profiles. Additionally, the preferential polyaromatic removal pathway of the Ni-MMO is clearly reflected in the curve shift to the right relative to CoMo-alumina-derived petcoke. This corresponds to an increase in higher oxidation temperature hydrocarbons.

Consequently, the difference in burnoff curves highlights the problems associated with subscription to the methodology in which a set temperature range is applied and the mass loss within this range is assumed to be the petcoke. This latter method has been widely used in earlier works and therefore fails to discriminate between the various elemental and structural properties of different petcoke types.[4,12,15] Consequently, this technique has limitations which can lead to unnecessary inaccuracies. Therefore, petcoke from each upgrading reaction type should be individually analyzed so that accurate inferences may be made about the elemental constituents and structure of the petcoke. Moreover, it has been highlighted previously that the TGA curves of spent hydroprocessing catalyst and asphaltenes extracted using the *n*-heptane solvent method (ASTM D3279) show oxidation in the same region which suggests TGA alone cannot be used to differentiate between the two components, asphaltene and coke.[34] This re-enforces the need for adequate toluene washing to remove the components that do not represent petcoke.

4. CONCLUSIONS

The challenges facing the refining of heavier oil feeds has led to the investigation of an alternative, economical catalyst. Catalytic upgrading was carried out in a stirred batch reactor, conditions of which were taken from a previously established optimization study relating specifically to the THAI-CAPRI method, an in situ thermal EOR incorporating a pelleted catalyst fixed-bed. A high-surface area Ni-enriched Mixed Metal Oxides (Ni-MMO) catalyst was used as an ultradispersed variation of the fixed-bed production liner, simulating upgrading with a different contacting pattern. The Ni-MMO was compared with a hydroprocessing catalyst, CoMo-alumina, and thermal upgrading under N_2 and H_2 atmospheres. The results show that the Ni-MMO catalyst condition was the most sensitive to the atmosphere composition. Ni-MMO (N_2) proved to generate the lowest liquid phase viscosity at 0.2 mPa·s coupled with the highest percentage of light napthas at 39.6%. Subsequent elemental analysis on the Ni-MMO (N_2) and -(H_2) derived petcoke has shown quantities of sulfur of 0.87 and 0.62 wt %, respectively. Ni-MMO (N_2) produced NiO following dehydration and dehydroxylation. This led to the formation of pseudopetcoke nuclei by providing adsorption sites for sulfur-rich poly aromatic components, stimulating a significant desulphurization pathway. This was accompanied by a significant increase in the gas and coke phases at 10.6 and 18.3%, respectively. Conversely, for Ni-MMO (H_2), the sulfur content of the coke decreased by 29.0% to a total 0.62 wt %. The presence of hydrogen partially reduced the catalyst, stimulating hydrogenation reactions which act to cap radical adducts and prevent the formation of mesophase. This is evidenced by the increase in liquid phase by 12.2% and a reduction of petcoke and gas phases to 6.4 and 13.8%, respectively. It is therefore clear that the introduction of a suitable hydrogen donor during THAI-CAPRI will increase the quantity of liquid phase. Furthermore, the refinery catalyst demonstrated the most significant reduction, by 37.6%, in liquid sulfur phase activity. However, with subsequent manipulation of both the LDH precursor and modification to the resultant Ni-MMO, an increased catalytic upgrading activity may pave the way for more economical and easily synthesized catalysts in the subsurface and surface refining industries.

AUTHOR INFORMATION

Corresponding Author

*Tel: +44 (0)1214145295. Fax: +44 (0)1214145324. E-mail: J.Wood@bham.ac.uk.

ORCID

Joseph Wood: 0000-0003-2040-5497

Notes

The authors declare no competing financial interest.

ACKNOWLEDGMENTS

The work contained in this paper was conducted during a PhD study undertaken as part of the Natural Environment Research Council (NERC) Centre for Doctoral Training (CDT) in Oil & Gas [grant number NEM00578X/1] and is funded by NERC and the School of Chemical Engineering at the University of

DOI: 10.1021/acs.energyfuels.9b02735
Energy Fuels 2019, 33, 10820−10832

Birmingham, whose support is gratefully acknowledged. Touchstone Exploration Inc, Canada, are thanked for supplying the heavy crude oil used in this study. The liquid phase sulfur analysis was outsourced to Exeter Analytical Limited (Coventry). The TPD and TPR analysis was performed by Dr. Helen Daly at the Department of Chemical Engineering and Analytical Science, University of Manchester.

REFERENCES

(1) BP. BP Energy Outlook 2018 edition. **2018**.
(2) Meyer, R. F., Attanasi, E. D., Freeman, P. A.. Heavy oil and natural bitumen resources in geological basins of the world. *US Geol Surv* **2007**; Open File-:36. DOI: 10.3133/ofr20071084.
(3) Xia, T. X.; Greaves, M. In situ upgrading of Athabasca Tar Sand bitumen using THAI. *Chem. Eng. Res. Des.* **2006**, *84*, 856−64.
(4) Al-Marshed, A.; Hart, A.; Leeke, G.; Greaves, M.; Wood, J. Optimization of Heavy Oil Upgrading Using Dispersed Nanoparticulate Iron Oxide as a Catalyst. *Energy Fuels* **2015**, *29*, 6306−16.
(5) EPA. Control of Air Pollution From Motor Vehicles: Tier 3 Motor Vehicle Emission and Fuel Standards AGENCY: Environmental Protect **2014**; 79.
(6) Cavani, F.; Trifirò, F.; Vaccari, A. Hydrotalcite-type anionic clays: Preparation, properties and applications. *Catal. Today* **1991**, *11*, 173−301.
(7) Clause, O.; Goncalves Coelho, M.; Gazzano, M.; Matteuzzi, D.; Trifirò, F.; Vaccari, A. Synthesis and thermal reactivity of nickel-containing anionic clays. *Appl. Clay Sci.* **1993**, *8*, 169−86.
(8) Mostafa, M. S.; Mohamed, N. H. Towards novel adsorptive nanomaterials: Synthesis of Co2+Mo6+ LDH for sulfur and aromatic removal from crude petrolatum. *Egypt. J. Pet.* **2016**, *25*, 221−7.
(9) Zhao, R.; Yin, C.; Zhao, H.; Liu, C. Synthesis, characterization, and application of hydotalcites in hydrodesulfurization of FCC gasoline. *Fuel Process. Technol.* **2003**, *81*, 201−9.
(10) Rana, M. S.; Sámano, V.; Ancheyta, J.; Diaz, J. A. I. A review of recent advances on process technologies for upgrading of heavy oils and residua. *Fuel* **2007**, *86*, 1216−31.
(11) Gray, M. R.. *Upgrading Oilsands Bitumen and Heavy Oil*. The University of Alberta Press: 2015.
(12) Hart, A.; Greaves, M.; Wood, J. fixed-bed and dispersed catalytic upgrading of heavy crude oil using-CAPRI. *Chem. Eng. J.* **2015**, *282*, 213−23.
(13) Hart, A.; Leeke, G.; Greaves, M.; Wood, J. Down-hole heavy crude oil upgrading by CAPRI: Effect of hydrogen and methane gases upon upgrading and coke formation. *Fuel* **2014**, *119*, 226−35.
(14) Hart, A.; Omajali, J. B.; Murray, A. J.; MacAskie, L. E.; Greaves, M.; Wood, J. Comparison of the effects of dispersed noble metal (Pd) biomass supported catalysts with typical hydrogenation (Pd/C, Pd/Al2O3) and hydrotreatment catalysts (CoMo/Al2O3) for in-situ heavy oil upgrading with Toe-to-Heel Air Injection (THAI). *Fuel* **2016**, *180*, 367−76.
(15) Brown, A. R.; Hart, A.; Coker, V. S.; Lloyd, J. R.; Wood, J. Upgrading of heavy oil by dispersed biogenic magnetite catalysts. *Fuel* **2016**, *185*, 442−8.
(16) Bi, W.; McCaffrey, W. C.; Gray, M. R. Agglomeration and deposition of coke during cracking of petroleum vacuum residue. *Energy Fuels* **2007**, *21*, 1205−11.
(17) Zarezadeh-Mehrizi, M, Afshar Ebrahimi, A, Rahimi, A. *Comparison of γ and δ-Al2O3 supported CoMo catalysts in the hydrodesulphurization of straight-run gas oil*. Sharif University of Technology 2019; *26*: 1555−1565. DOI: 10.24200/sci.2019.50969.1948.
(18) IHS. Light and Heavy Naphtha: International Market Analysis. 2017.
(19) Hunter, K. C.; East, A. L. L. Properties of C-C Bonds in n-Alkanes: Relevance to Cracking Mechanisms. *J. Phys. Chem. A* **2002**, *106*, 1346−56.
(20) Hart, A.; Lewis, C.; White, T.; Greaves, M.; Wood, J. Effect of cyclohexane as hydrogen-donor in ultradispersed catalytic upgrading of heavy oil. *Fuel Process. Technol.* **2015**, *138*, 724−33.
(21) Franco, C.; Patiño, E.; Benjumea, P.; Ruiz, M. A.; Cortés, F. B. Kinetic and thermodynamic equilibrium of asphaltenes sorption onto nanoparticles of nickel oxide supported on nanoparticulated alumina. *Fuel* **2013**, *105*, 408−14.
(22) Hart, A.; Shah, A.; Leeke, G.; Greaves, M.; Wood, J. Optimization of the CAPRI process for heavy oil upgrading: Effect of hydrogen and guard bed. *Ind. Eng. Chem. Res.* **2013**, *52*, 15394−406.
(23) Javadli, R.; De Klerk, A. Desulfurization of heavy oil-oxidative desulfurization (ODS) as potential upgrading pathway for oil sands derived bitumen. *Energy Fuels* **2012**, *26*, 594−602.
(24) Mckenna, A. M.; Marshall, A. G.; Rodgers, R. P. Heavy Petroleum Composition. 4. *Energy Fuels* **2013**, *27*, 1257.
(25) Hart, A. The novel THAI-CAPRI technology and its comparison to other thermal methods for heavy oil recovery and upgrading. *J. Pet. Explor. Prod. Technol.* **2014**, *4*, 427−37.
(26) Gateau, P.; Hénaut, I.; Barré, L.; Argillier, J. F. Heavy Oil Dilution. *Oil Gas Sci. Technol.* **2004**, *59*, 503−9.
(27) Ilyin, S.; Arinina, M.; Polyakova, M.; Bondarenko, G.; Konstantinov, I.; Kulichikhin, V.; et al. Asphaltenes in heavy crude oil: Designation, precipitation, solutions, and effects on viscosity. *J. Pet. Sci. Eng.* **2016**, *147*, 211−7.
(28) Franco, C. A.; Nassar, N. N.; Montoya, T.; Ruíz, M. A.; Cortés, F. B. Influence of asphaltene aggregation on the adsorption and catalytic behavior of nanoparticles. *Energy Fuels* **2015**, *29*, 1610−1621.
(29) Siskin, M.; Kelemen, S. R.; Gorbaty, M. L.; Ferrughelli, D. T.; Brown, L. D.; Eppig, C. P.; et al. Chemical approach to control morphology of coke produced in delayed coking. *Energy Fuels* **2006**, *20*, 2117−24.
(30) Ibrahim, H. A. Thermal Treatment of Syrian Shot Coke. *Recent Advances in Petrochemical Science (RAPSCI)* **2017**, *2*, 1−5.
(31) Zhang, H.; Chen, J.; Guo, S. Preparation of natural gas adsorbents from high-sulfur petroleum coke. *Fuel* **2008**, *87*, 304−11.
(32) Lakhova, A.; Petrov, S.; Ibragimova, D.; Kayukova, G.; Safiulina, A.; Shinkarev, A.; et al. Aquathermolysis of heavy oil using nano oxides of metals. *J. Pet. Sci. Eng.* **2017**, *153*, 385−90.
(33) Birghila, S., Carazeanu, I.. Evaluation of the Physical-Chemical Properties in Petroleum Coke **2013**;*6*:28−31 .
(34) Barman, B. N.; Skarlos, L.; Kushner, D. J. Simultaneous determination of oil and coke contents in spent hydroprocessing catalyst by thermogravimetry. *Energy Fuels* **1997**, *11*, 593−5.

NOTE ADDED AFTER ASAP PUBLICATION

This article published November 1, 2019 with an error in the title of Table 4. The correct title published November 6, 2019.

DOI: 10.1021/acs.energyfuels.9b02735
Energy Fuels 2019, 33, 10820−10832